European Journal of Pharmaceutics and Biopharmaceutics 73 (2009) 324–330

Contents lists available at ScienceDirect

European Journal of Pharmaceutics and Biopharmaceutics

journal homepage: www.elsevier.com/locate/ejpb

Research paper

Alteration of the glycosylation pattern of monocytic THP-1 cells upon differentiation and its impact on lectin-mediated drug delivery

V.E. Plattner, G. Ratzinger, E.T. Engleder, S. Gallauner, F. Gabor, M. Wirth *

Department of Pharmaceutical Technology and Biopharmaceutics, University of Vienna, Vienna, Austria

ARTICLE INFO

Article history:
Received 24 February 2009
29 June 2009
Accepted in revised form 8 July 2009
Available online 12 July 2009

Keywords:
Monocytes/macrophages
Glycosylation pattern
Lectins
Bioadhesion
Drug targeting
Nanoparticles

ABSTRACT

In the present study, human monocytic THP-1 cells were treated with phorbol-12-myristate-13-acetate (PMA) in order to obtain macrophage-like cells. Before and after treatment, plant lectins with distinct sugar specificities were applied in order to elucidate the glycosylation patterns of both monocytic and macrophage-like cell types and to follow changes during differentiation.

As a result of flow-cytometric analyses, for untreated as well as for PMA-differentiated cells WGA yielded the highest binding rate without significant changes in the binding capacity. For the other lectins, divergent results were obtained which point to reorganization of sugar residues on the cell surface during differentiation.

Additionally, cytoinvasion being beneficial for enhanced drug absorption was studied with WGA which had displayed a high binding capacity together with a high specificity. For both untreated and PMA-differentiated cells decreased fluorescence intensity at 37 °C as compared to 4 °C was observable pointing to internalization and accumulation within acidic compartments. Moreover, WGA-functionalized PLGA nanoparticles were prepared, and their uptake evaluated. Uptake rates of 55% in case of PMA-differentiated cells suggested that WGA-grafted drug delivery systems might be an interesting approach for treatment of infectious diseases provoked by parasites, facultative intracellular bacteria, or viruses such as HIV.

1. Introduction

Being essential parts of the immune system, monocytes and macrophages are involved in defense against microbial infection, initiation of inflammation, immunity to foreign substances, wound healing, and angiogenesis. They originate from the bone marrow and undergo differentiation from hematopoietic stem cells to blood monocytes and finally to tissue-specific macrophages. Like all eukaryotic cells, they are covered by a carbohydrate-rich layer, denominated glycocalyx or pericellular matrix [1,2]. This cell coat is several tens of nanometers thick and is of functional importance as the first line defense of the innate immune system is relying on recognition of carbohydrates [3]. Furthermore, it plays an important role in cell–cell and cell–matrix interactions. At this, there is evidence that glycocalyx elements influence the endocytic capacity of monocytes [4] and are modulated during adhesion [5,6]. As adhesion of peripheral blood monocytes to endothelial cells initiates the differentiation program of monocytes into phagocytes [7], this process may also cause reorganization of sugar residues at the cell surface.

To investigate the glycosylation pattern of monocytes, which undergo differentiation to macrophages, the human monocytic leukemia cell line THP-1 was chosen, which was established by Tsuchiya et al. and exhibits stable monocytic characteristics [8]. Additionally, treatment with various agents such as DMSO, phorbol-12-myristate-13-acetate (PMA), 1, 25-dihydroxyvitamin D3 (VD3), retinoic acid, or cytokines results in differentiation along the monocytic lineage [9–11]. In summary, it was shown that macrophage-like cells, which mimic native monocyte-derived macrophages in several aspects, are obtained with phorbol esters [12], whereas DMSO or retinoic acid shift the cells rather to characteristics of neutrophils [13].

In the present study, differentiation was carried out with PMA according to Park et al. [14]. In comparison to primary human monocytes, THP-1 cells are characterized by homogeneity, accessibility, and a higher transfection efficiency which renders them a reliable cell model.

To identify and characterize the glycocalyx elements of both untreated and PMA-differentiated THP-1 cells, binding of fluorescent-labeled lectins was investigated. Lectins represent carbohydrate-binding proteins which recognize distinct sugar structures at the cell surface. In order to cover a broad range of sugar residues at

* Corresponding author. Department of Pharmaceutical Technology and Biopharmaceutics, University of Vienna, A-1090 Vienna, Austria. Tel.: +43 1 4277 55407; fax: +43 1 4277 9554.
E-mail address: michael.wirth@univie.ac.at (M. Wirth).

0939-6411/$ - see front matter © 2009 Elsevier B.V. All rights reserved.
doi:10.1016/j.ejpb.2009.07.004

the cell surface, several plant lectins with diverse carbohydrate specificities were applied: wheat germ agglutinin (WGA) and *Solanum tuberosum* lectin (STL) were used to identify *N*-acetyl-D-glucosamine structures and in case of WGA also sialic acid residues can be detected. The lectin from *Sambucus nigra* (SNA) specifically recognizes sialic acid (2,6)Gal/GalNAc sequences, and *Lens culinaris* agglutinin (LCA) binds to mannose residues. Peanut agglutinin (PNA) was used to detect galactosamine moieties, *Dolichus biflorus* agglutinin for *N*-acetyl-D-galactosamine-containing structures, and *Ulex europaeus* isoagglutinin I (UEA) specifically binds to fucose.

Ongoing from this characterization and comparison of the pericellular matrices of both untreated and PMA-differentiated cells, the internalization of WGA was studied in detail. This lectin had already been shown to enhance the phagocytic and bactericidal activity of murine peritoneal macrophages [15], and hence might be a suitable candidate for advanced drug delivery purposes. As improved drug delivery might promise higher therapeutic efficiency together with a reduction in side effects, there are considerable efforts to identify appropriate "targeters" which can be used for the functionalization of drug delivery devices. Therefore, nanoparticles were prepared from the biocompatible and biodegradable polymer poly(DL-lactide-co-glycolide) (PLGA) and surface modified with WGA [16]. Subsequently, their interaction with untreated and PMA-differentiated THP-1 cells was studied in order to examine the potential of WGA for guiding nanoparticles to macrophages.

2. Materials and methods

2.1. Chemicals

Fluorescein-labeled lectins from *Triticum vulgare* (wheat germ agglutinin (WGA); molar ratio fluorescein/protein (F/P) = 2.9), *Solanum tuberosum* (STL; F/P = 3.1), *Sambucus nigra* (SNA, F/P = 7.2), *Lens culinaris* (LCA; F/P = 3.8), *Arachis hypogaea* (peanut agglutinin (PNA); F/P = 5.2), *Dolichos biflorus* (DBA; F/P = 2.2), and *Ulex europaeus* (UEA; F/P = 2.7) were purchased from Vector Laboratories (Burlingame, CA, USA). For the immunofluorescence analysis, FITC-labeled antibodies were obtained from Beckman Coulter (Krefeld, Germany). For particle preparation, poly(DL-lactide-co-glycolide) RESOMER® RG 503 H (PLGA) was purchased from Boehringer Ingelheim (Ingelheim, Germany). All other chemicals were purchased from Sigma (St. Louis, MO, USA) unless otherwise specified.

2.2. Cell culture

Human THP-1 monocytic leukemia cells were obtained from the American Type Culture Collection (Manassas, VA, USA). Cells were seeded at a density of 1×10^5 cells/ml in RPMI-1640 medium containing 10% heat-inactivated FCS (Biochrom AG, Berlin, Germany), 200 mM L-glutamine, 10,000 U/ml penicillin, and 10,000 μg/ml streptomycin and maintained at 3–8 $\times 10^5$ cells/ml in a humidified atmosphere with 5% CO_2 at 37 °C.

Differentiation into macrophages was achieved by resuspending the cells at 3×10^5 cells/ml in growth medium supplemented with phorbol-12-myristate-13-acetate (PMA; 8 nM in DMSO) for 48 h. To analyse the surface marker CD14 by immunofluorescence, cells were incubated with PMA also for 24 h and 72 h.

Viability of the cells was determined by trypan blue exclusion and counting the viable cells using a Bürker-Türk hemocytometer. Adherence of PMA-differentiated cells was examined with the same setup by determining the amount of unattached and adherent cells. Unattached cells were collected by centrifugation (1000 rpm, 5 min, 4 °C) of the supernatant, whereas adherent cells were detached with 0.25% EDTA in PBS followed by centrifugation.

2.3. Immunofluorescence analysis of surface antigen CD14

Untreated THP-1 cells were harvested by centrifugation (1000 rpm, 5 min, 4 °C) and resuspended in RPMI medium at a concentration of 5×10^6 cells/ml. PMA-differentiated cells were detached and collected as described above and resuspended at the same concentration as untreated cells.

A cell suspension of 50 μl (5×10^6 cells/ml) was incubated with 210 μl of the FITC-labeled anti-human CD14 monoclonal antibody solution (MY4-FITC, diluted 1:20 in PBS with 2% FCS) for 30 min at 4 °C. After incubation, cells were spun down (1000 rpm, 5 min, 4 °C) and the supernatant was discarded. Then, 100 μl PBS was added, and this washing step was repeated to remove any unbound antibody. Finally, cells were resuspended in 1 ml particle free PBS, and the mean cell-associated fluorescence intensity (MFI) was determined by flow cytometry (Epics XL-MCL, Coulter, FL, USA). To detect any non-specific antibody binding, additional cells were treated with an adequate isotypic control (MsIgG2b-FITC) or with PBS before analysis.

2.4. Lectin-binding capacity

Untreated and PMA-differentiated cells were harvested as described earlier and processed immediately. A cell suspension of 50 μl (5×10^6 cells/ml) was incubated with a dilution series of fluorescein-labeled lectins (3.125–100 pmol in PBS, 50 μl) for 15 min at 4 °C. Then, cells were washed and prepared for flow cytometry as described above. Negative controls containing PBS instead of the lectin solution were included in all experiments and considered for all calculations. As a control to estimate non-specific-binding, samples were prepared as described above but using a dilution series of fluorescein-labeled bovine serum albumin (BSA, (F/P = 10)) instead of the lectins.

2.5. Specificity of the lectin binding

To determine if the binding of the lectins is mediated by carbohydrate moieties at the surface of untreated and PMA-differentiated THP-1 cells, 50 μl cell suspension (5×10^6 cells/ml), 100 μl of a dilution series of the corresponding complementary carbohydrate, and 50 μl of a solution containing 12.5 pmol fluorescein-labeled lectin were incubated for 15 min at 4 °C. The subsequent processing was again performed as described above. Table 1 displays the respective inhibitory carbohydrate for each lectin and the amounts used in the study. According to preliminary results, UEA-I and DBA exhibited no binding to either untreated or PMA-differentiated cells. Hence, no specificity studies were carried out for these lectins. The specificity of the interaction between SNA and THP-1 cells was not determined as the corresponding carbohydrate sialic acid α2,6 Gal/GalNAc is commercially unavailable.

2.6. Internalization of surface-bound WGA

To evaluate the internalization of surface-bound WGA, 50 μl cell suspension (5×10^6 cells/ml) of untreated and PMA-differentiated cells were incubated with 50 μl WGA solution containing 12.5 pmol lectin for 15 min at 4 °C (pulse incubation). Unbound lectin was removed by centrifugation and washing with 150 μl PBS. Subsequently, cells were further incubated for 0–240 min at either 4 °C or 37 °C (chase incubation) and then prepared for flow cytometry. After determination of the mean fluorescence intensity (MFI), 40 μl monensin solution (2.4 mM in EtOH) was added, and cells were incubated for 3 min at room temperature. Finally, the MFI was assessed again.

Table 1
Specificity of the lectins used in the competitive-binding assays.

Lectin	MW	Carbohydrate specificity	Inhibitory sugar	Sugar [c] in μmol/reaction (untreated/differentiated)
WGA	36,000	GlcNAc, sialic acid	*N*-acetyl-D-glucosamine, Chitotriose	0.004–0.125/0.004–0.125
STL	100,000	GlcNAc	*N*-acetyl-D-glucosamine, Chitotriose	0.004–0.125/0.004–0.125
PNA	110,000	ß-D-Gal-D-GalNAc, ß-D-GalNAc, Gal	D-galactosamine	0.031–1/n.d.
DBA	120,000	α-D-GalNAc, Gal	*N*-acetyl-D-galactosamine	n.d./n.d.
UEA	63,000	α-L-Fuc	L-fucose	n.d./n.d.
SNA	150,000	Sialic acid α(2,6)Gal/GalNAc	–	n.d./n.d.
LCA	49,000	α-Man, α-Glc, α-GlcNAc	D-mannose	n.d./1–32

GlcNac, *N*-acteyl-D-glucosamine; α-Glc, α-glucose; α-D-GalNAc, *N*-acetyl-α-galactosamine; Gal, galactose; α-L-Fuc, α-L-fucose; α-Man, α-mannose; and n.d., not determined.

2.7. Preparation of WGA-functionalized nanoparticles

Nanoparticles were prepared by the solvent evaporation technique. Briefly, 400 mg of PLGA was dissolved in 2 g ethyl acetate. Upon addition of 6 ml 10 % (w/w) aqueous solution of Pluronic® F68, the organic phase was dispersed in the aqueous phase by ultrasonication for 50 s (Bandelin electronic Sonopuls UW 70/HD 70, tip MS 72/D, Berlin, Germany). The resulting O/W emulsion was poured into 100 ml 1% (w/w) aqueous solution of Pluronic® F68. The organic solvent was allowed to evaporate at room temperature during mechanical stirring (600 rpm) at atmospheric pressure for 1 h and subsequently during 1 h under reduced pressure.

The PLGA nanospheres were covalently coupled with fluorescein-labeled WGA or fluorescein-labeled BSA. For this purpose, 40 ml of the particle suspension was activated by addition of 480 mg N-(3-dimethylaminopropyl)-N′-ethylcarbodiimide hydrochloride (EDAC) and 20 mg N-hydroxysuccinimide (NHS), each dissolved in 1 ml of 20 mM HEPES/NaOH buffer pH 7.4. After end-over-end incubation for 2 h at room temperature, the suspension was washed twice by diafiltration (Vivaflow 50, 100 000 MWCO PES, Sartorius Vivascience GmbH, Goettingen, Germany) using 80 ml of 0.1% Pluronic in 20 mM HEPES/NaOH pH 7.4. The nanoparticle suspension was divided into two equal parts followed by addition of 20 nmol of WGA (0.72 mg) and BSA (1.32 mg), respectively, each dissolved in 1 ml of the same buffer as described earlier. Following end-over-end incubation overnight at room temperature non-reacted coupling sites were saturated by addition of 300 mg glycine to each tube and further incubation for 1 h. Finally, excess of reagents was removed by three cycles of diafiltration with 40 ml of 0.1% Pluronic in 20 mM isotonic HEPES/NaOH pH 7.4 each. The amount of fluorescein-labeled protein coupled to the particle surface was determined by fluorimetric analysis following dissolution of an aliquot in 0.1 M NaOH. The respective nanosphere suspensions contained 3.9 μg/ml WGA and 2.2 μg/ml BSA coupled to the particle surface. The concentration of the nanoparticle suspension amounted to 1.2 mg PLGA/ml. The mean particle size as determined by dynamic light scattering (Zetasizer Nano ZS, Malvern Instruments Ltd., UK) was 160.3 nm for WGA-functionalized nanospheres with a polydispersity index (PDI) of 0.130 and 151.2 nm for BSA-coated nanospheres with a PDI of 0.133 using 0.1% Pluronic in 20 mM isotonic HEPES/NaOH pH 7.4 as dispersant.

2.8. Internalization of surface-bound WGA-functionalized PLGA nanoparticles

In order to examine the interaction between WGA- or BSA-coupled PLGA nanospheres and untreated as well as PMA-differentiated THP-1 cells, 50 μl cell suspension (5×10^6 cells/ml) was incubated with 50 μl nanoparticle suspension (1.2 mg PLGA/ml) for 15 min at 4 °C (pulse incubation). Unbound particles were removed as described above, and the cells were further incubated for 30, 60 or 120 min at either 4 °C or 37 °C (chase incubation). After a first flow-cytometric analysis, 40 μl monensin (2.4 mM in EtOH) was added. Thereupon, cells were incubated for 3 min at room temperature, and the MFI values were determined again.

2.9. Flow cytometry

Data were acquired using an Epics XL-MLC analytical flow cytometer (Coulter, FL, USA). In order to exclude any dead cells, debris, and aggregates, viable cells were gated according to their forward versus side scatter properties. From each sample, 3000 cells were accumulated within this gate. Fluorescence emission of the fluorescence labeled single cell-population was measured at 525 nm (10 nm bandwidth) after excitation at 488 nm. Data analysis was conducted using Coulter System II Software 3.0.

2.10. Fluorescence microscopy

Uptake of WGA-functionalized PLGA nanoparticles was visually confirmed by incubating 50 μl cell suspension (5×10^6 cells/ml, both untreated and PMA-differentiated cells) with 50 μl nanoparticle suspension for 15 min at 4 °C (pulse incubation). After removal of unbound particles as described above, the cells were further incubated for 120 min at 37 °C. Thereafter, cells were washed again and immediately mounted for microscopy without fixation. Control samples were incubated at 4 °C only.

Immunofluorescence images were obtained using a Nikon Eclipse 50i microscope equipped with an EXFO X-Cite 120 fluorescence illumination system. Excitation and emission filter blocks were at 465–495/515–555 for green fluorescence and 510–560/>590 for red fluorescence. Fluorescence images were acquired at 40× magnification and processed using Lucia G v5.0 software for image evaluation.

2.11. Statistics

Statistical analyses were carried out using the Microsoft Excel® integrated analysis tool. The hypothesis test among two data sets was made by comparing two means from independent (unpaired) samples (*t*-test). Values of $p < 0.05$ were considered significant. All experiments were performed at least in triplicate.

3. Results

3.1. PMA-induced differentiation of THP-1 monocytes to macrophages

After treatment of THP-1 cells with 8 nM PMA for 48 h, adherence and morphology were examined microscopically. Analysis of cell adherence by counting after trypan blue exclusion revealed that >90% of the cells were attached to the surface after PMA treatment. Additionally, adherent THP-1 cells were more flattened and elongated indicating the macrophage phenotype as compared to

the untreated cells which remained round and in suspension albeit partly aggregated in clusters.

To further ensure differentiation to macrophages, CD14 expression was investigated as the up-regulation of this surface molecule has been reported for maturating monocytes [10,17]. Flow cytometric analysis revealed an increase in CD14 as compared to untreated THP-1 cells. The mean cell-associated fluorescence intensity (MFI) was 0.5 ± 0.3 in case of untreated cells, 0.8 ± 0.0 MFI for cells treated for 24 h, 9.9 ± 0.5 for cells treated for 48 h, and 26.0 ± 0.5 MFI in case of cells treated for 72 h. MFI values of the isotype control were 0.52 in case of untreated cells and 0.57 in case of PMA-differentiated cells and subtracted from all data quoted.

3.2. Lectin-binding capacity of THP-1 cells

Plant lectins with different carbohydrate specificities were used to estimate the glycosylation pattern of untreated and PMA-differentiated THP-1 cells. For comparison of the data, MFI values of each lectin were related to an apparent conjugation number of 1 mol fluorescein per mole of lectin. For both untreated and PMA-differentiated THP-1 cells, WGA yielded the highest binding capacity with MFI values between 1.0 ± 0.0 and 17.1 ± 0.2 (untreated cells) and 0.7 ± <0.1 and 16.6 ± 0.4 (PMA-differentiated cells), respectively (Fig. 1). In case of untreated THP-1 cells, lectin binding was also observed for STL (MFI values up to 10.3 ± 0.5), PNA (up to 1.0 ± 0.1), and SNA (up to 0.3 ± <0.1) (Fig. 1A). LCA revealed only very low MFI values scarcely above the autofluorescence of the cells (0.1 ± <0.1). For both untreated and PMA-differentiated cells, binding of UEA-I, DBA as well as BSA, which served as a control for non-specific protein-membrane interactions, was not detectable. Comparison of the two different THP-1 types exhibited for PMA-differentiated THP-1 cells also a distinct interaction with STL (MFI values up to 5.8 ± 0.2) and SNA (1.2 ± <0.1) (Fig. 1B). Interestingly, a notably higher interaction occurred with LCA (2.4 ± <0.1 MFI at 100 pmol) as compared to untreated THP-1 cells, whereas no binding of PNA was observed. Fig. 2 compares the results at a lectin concentration of 100 pmol. At this concentration, no significant differences ($p > 0.05$) were evaluated for WGA, as contrary to all other lectins ($p < 0.01$).

3.3. Specificity of the lectin–THP-1 interaction

The specificity of the interaction between the plant lectins and THP-1 cells was elucidated by competitive inhibition with complementary carbohydrates (Table 1). For both untreated and PMA-differentiated cells, addition of increasing amounts of corresponding carbohydrates resulted in a decrease in the cell-bound lectin. The results are shown exemplarily for PMA-differentiated cells in Fig. 3 and indicate the specificity of the lectin–cell interactions. Based on the control sample without any sugar addition representing 100%, the percentage of inhibition was calculated. At this, inhibition values of more than 85% were calculated for WGA, STL, and LCA which point to a highly specific interaction of the respective lectin with cellular structures. In case of untreated cells, similar results were obtained for WGA and STL with inhibition values of about 90% in the same concentration range (data not shown). As LCA had not shown a relevant binding capacity to untreated THP-1, the specificity of the PNA–cell interaction was assessed instead, which also turned out to be specific as represented by more than 90% inhibition at a concentration of 1 μmol galactosamine/reaction (data not shown).

3.4. Internalization of surface-bound WGA

Fig. 4 depicts the results of the internalization experiments with PMA-differentiated THP-1 cells. After pulse incubation at 4 °C, the MFI values of surface-bound WGA amounted to 41.5 ± 0.9 at the mean. During chase incubation at 37 °C, a time-dependent decrease in fluorescence intensities was observed resulting in 15.8 ± 0.5 MFI after 240 min. In case of untreated THP-1 cells (data not shown), MFI values yielded 40.6 ± 2.0 after pulse incubation and decreased to 14.2 ± 1.1 upon incubation at 37 °C for 240 min. After adding monensin to these WGA pretreated cells, the reduced fluorescence intensity was restored and approached the same level as the control samples at 4 °C. In addition, the same assays were performed for both untreated and PMA-differentiated cells also at 4 °C where no considerable differences were observable between the MFI values prior and after monensin additions.

3.5. Interaction of WGA-functionalized nanoparticles with THP-1 cells

To investigate a potential applicability of lectins for directing drugs to macrophages, the interaction of WGA-functionalized nanoparticles with THP-1 cells was studied. After a pulse incubation at 4 °C and removal of unbound particles, the chase incubation was performed up to 120 min at 4 °C and 37 °C. During chase incubation of untreated cells at 37 °C, MFI values decreased from 9.1 ± 0.4 (0 min) to 6.0 ± 0.1 (120 min). Upon addition of monensin, the cell-bound fluorescence intensity was restored by reaching 9.1 ± 0.5 (120 + 3 min monensin). In case of PMA-differentiated cells, the MFI values declined from 5.7 ± 0.4 (0 min) to 3.2 ± 0.2 (120 min) and re-equilibrated to 5.9 ± 0.2 (120 + 3 min monensin) upon addition of monensin. Chase incubation at 4 °C yielded stable MFI values for both untreated and PMA-differentiated cells.

In contrast, cell binding of BSA-conjugated nanospheres was near to the detection limit. The pulse incubation yielded MFI values of 0.1 ± <0.1 (untreated cells) and 0.2 ± 0.1 (PMA-differentiated cells) which are only marginally higher than the autofluorescence of the cells.

Additional information concerning the uptake of WGA-functionalized nanoparticles to untreated and PMA-differentiated THP-1 cells was collected via fluorescence microscopy. As illustrated in Fig. 5 for PMA-differentiated cells, control samples incubated with WGA at 4 °C revealed merely a fluorescent ring of particles around the cells indicating surface binding without any signs of internalization when the focus plane was set to the middle of the cell. In contrast, after incubation at 37 °C a dot-like pattern of fluorescence around the nucleus (black spot) was observed pointing to uptake and vesicular enrichment of initially surface-bound particles. For untreated cells, similar images were acquired (data not shown).

4. Discussion

In this study a systematic characterization of the glycosylation pattern of untreated and PMA-differentiated THP-1 cells was performed via detailed analysis of the binding capacities of selected lectins in order to investigate possible changes in course of the differentiation process. Additionally, the potential applicability of the applied lectins for drug delivery purposes at both stages was elucidated. For untreated as well as for PMA-differentiated THP-1 cells, the highest binding capacity was found for WGA, a lectin specific for *N*-acetyl-D-glucosamine and sialic acid structures. Regarding the MFI values at 100 pmol, no significant difference ($p > 0.05$) between both untreated and PMA-differentiated cells was detected. STL was the second best binding lectin for both untreated and PMA-differentiated cells, which also recognizes *N*-acetyl-D-gluco-

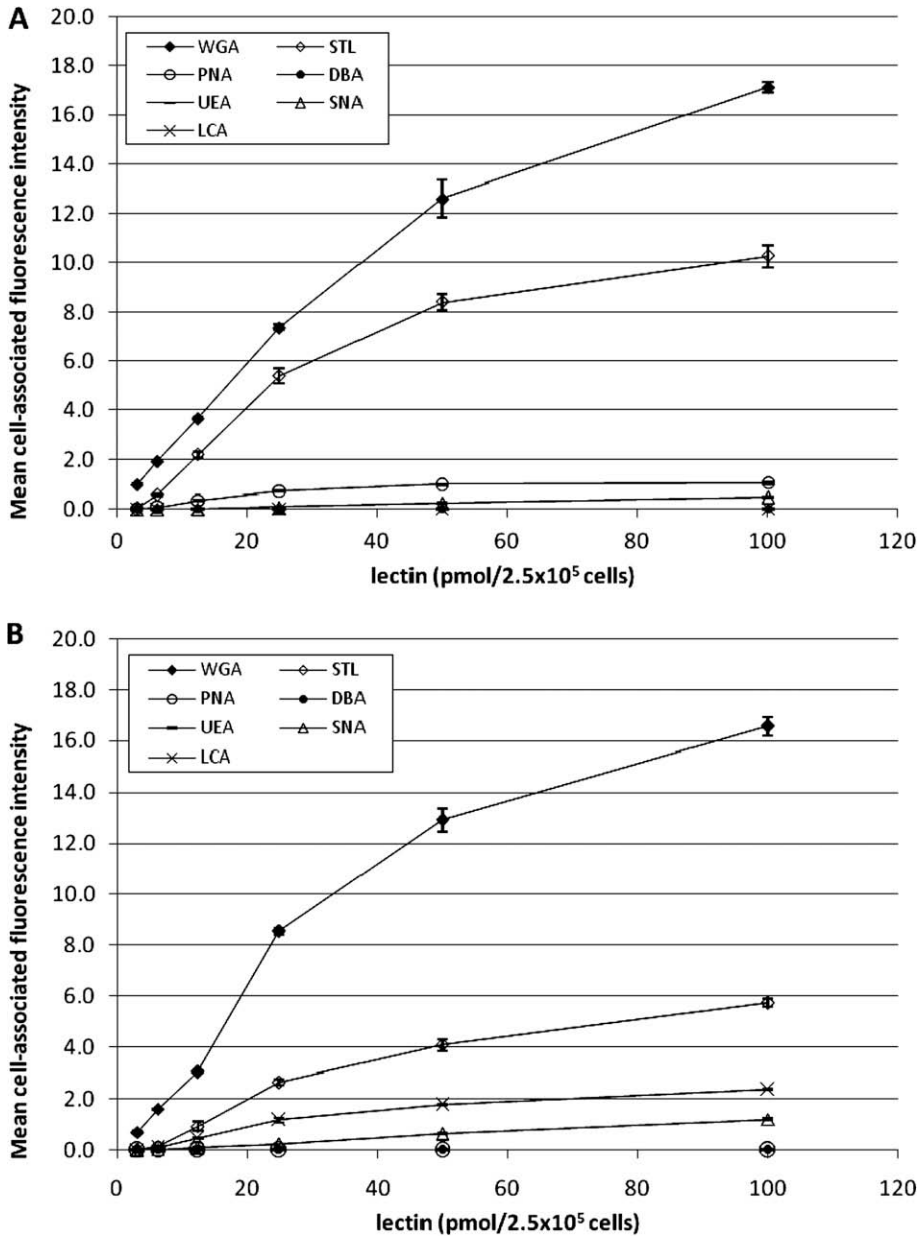

Fig. 1. Lectin binding to undifferentiated THP-1 (A) and differentiated THP-1 cells (B) at 4 °C. The fluorescein-labeled lectins associated with the cell surface were related to an apparent F/P ratio of 1 (mean ± SD, $n = 3$).

samine residues. In contrast to WGA, STL binding was significantly different between PMA-differentiated and untreated cells over the whole concentration range tested. This decrease in *N*-acetyl-D-glucosamine residues might be attributed to an increase in sialic acid moieties present at the cell surface of PMA-differentiated cells as indicated by the binding rate of SNA, a lectin which specifically binds to α2,6-linked sialyl groups and yielded a higher binding capacity in case of PMA-differentiated THP-1 cells too ($p < 0.01$). Significant differences in the lectin-binding pattern were also observed for PNA and LCA. In case of untreated cells, galactosamine residues were assessed via PNA, whereas PMA-differentiated cells only showed a PNA binding scarcely above the autofluorescence level. In contrast, binding of LCA to mannose structures was very low in case of untreated cells, whereas PMA-differentiated cells revealed a notably higher density of mannose at the cell surface. Accessible fucose residues, traceable via UEA, and *N*-acetyl-D-galactosamine moieties, being detectable with DBA, were neither found on monocytes nor on monocyte-derived macrophages.

Sabri et al. [6] demonstrated that increased adhesiveness of stimulated THP-1 cells resulted in decreased cell coat thickness, presumably mostly affecting O-linked carbohydrates. Since Galß1-3-GalNAc represents the core 1 structure of the O-linked chains and is detected by PNA binding, the loss of PNA-binding capacity upon differentiation of THP-1 cells to macrophages is in agreement with the aforementioned observation. Additionally, PMA differentiation also had an effect on N-linked sugar residues. Among the motifs on N-linked oligosaccharides, α2, 6-linked sialyl groups detectable by SNA and trimannosyl core groups detectable by LCA are present. For both lectins, a significantly higher binding capacity was determined on PMA-differentiated cells as compared to untreated ones ($p < 0.01$) which might be due to up-regulation of the CD14 receptor expression during differentiation. CD14 possesses four potential N-linked glycosylation sites with a carbohydrate content contributing to 20% of the total molecular mass [18]. Thus, increased binding of SNA and LCA might occur via these partial structures.

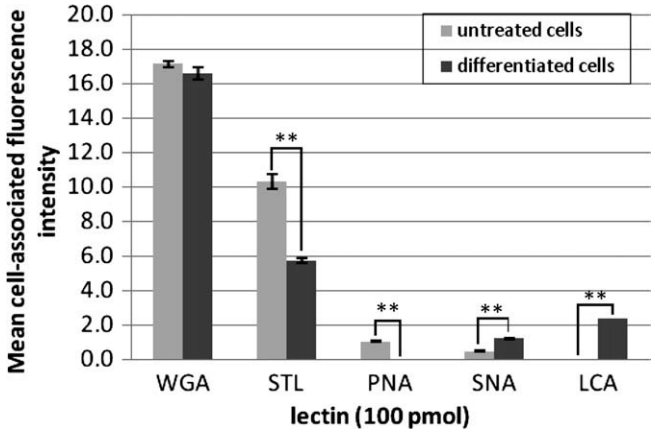

Fig. 2. Comparison of the lectin-binding capacities of untreated and differentiated THP-1 cells using a lectin concentration of 100 pmol (mean ± SD, $n = 3$). Statistically significant differences were determined by student's t-test: ** = $p < 0.01$.

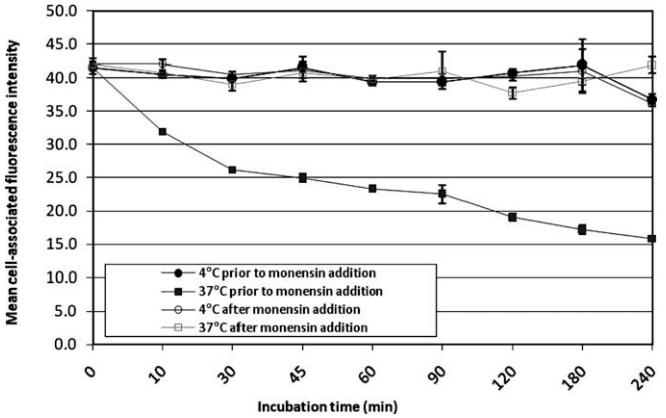

Fig. 4. Mean cell-associated fluorescence intensities of WGA-loaded differentiated THP-1 cells prior and after monensin additions during incubation (0–240 min) at both 4 °C and 37 °C (mean ± SD, $n = 3$).

For improved drug delivery purposes, not only a high binding rate, but also the specificity of the interaction is an important parameter. Thus, specificity of lectin binding was ascertained yielding inhibition values of at least 85% for each individual lectin.

Uptake of the "targeter", a favourable feature in advanced drug delivery, was observed for WGA. For this lectin, the enhancement of the phagocytic and bactericidal activities had been demonstrated with murine macrophages [15]. In our studies, WGA displayed a high binding capacity together with a high specificity for both untreated and PMA-differentiated THP-1 cells. In case of a selective approach towards either monocytes or macrophages, LCA might be a suitable candidate, as this lectin interacted only with PMA-differentiated THP-1 cells. On the contrary, PNA appears to be useful to target monocytic cells. However, according to a study with murine peritoneal macrophages, this lectin diminished the phagocytic activity suggesting that O-glycosylation is altered during activation of the cells [19]. This observation correlates with our results, and thus, its application as a targeting moiety is questionable.

The cellular fate of WGA was investigated over a period of 4 h at 4 °C and 37 °C, respectively. As shown in Fig. 5, the incubation temperature exerted a significant influence on the MFI values: upon chase incubation at 4 °C, they remained constant indicating an irreversible binding without any evidence for detachment or internalization of the cell-bound lectin. In contrast, at 37 °C the fluidity of the cell membrane increases and active transport processes can occur. Regarding the MFI values of WGA at this temperature, the observed continuous decrease points to internalization of the lectin and enrichment within acidic compartments, since the fluorescence emission of fluorescein is known to be reduced at acidic pH. Thus, monensin, a carboxylic ionophore which can compensate the pH gradient between the cytoplasma and acidic compartments was added to the cells to verify this assumption. After monensin treatment, the MFI could be re-established, and it underlines the obviously pH dependent and reversible quench of the acid-sensitive label (Fig. 5). As analyses of the supernatants yielded no detached WGA, calculation of the fraction of WGA entering the lysosomal pathway was possible [20]. In case of untreated THP-1 cells, about 15% of the surface-bound WGA were accumulated after 10 min, in case of PMA differentiated cells, it was 25%. The cytoinvasion of WGA at the end of incubation after 240 min amounted to 64% in case of untreated THP-1 cells and 74% in case of PMA-differentiated THP-1 cells, respectively. These results indicate that PMA treatment of THP-1 cells might elicit a faster and higher phagocytic activity. Nevertheless, for both untreated and PMA-differentiated cells, a high internalization rate was assessed, and thus, WGA seems to be an appropriate candidate for guiding drug carriers to differentiated as well as non-differentiated cells.

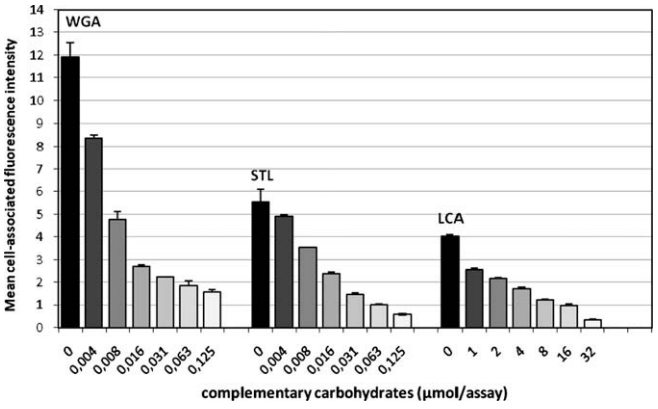

Fig. 3. Competitive inhibition of lectin binding (WGA, STL, LCA) to differentiated THP-1 cells by addition of increasing amounts of complementary carbohydrate (mean ± SD, $n = 3$).

Moreover, not only uptake of free WGA was observed, but also internalization of WGA-functionalized PLGA nanoparticles of about 160 nm in diameter. Again, incubation at 4 °C revealed stable MFI values, whereas incubation at 37 °C resulted in a decrease in cell-associated fluorescence intensities by time which could be restored upon addition of monensin. Regarding untreated cells, after 120 min about 40% of the surface-bound WGA-grafted particles were internalized and were subject to reversible pH quenching. Regarding PMA-differentiated cells, at the same time about 55% were taken up into acidic compartments. For comparison, the cell binding of BSA-grafted nanoparticles was assessed, but only marginal cell binding could be observed for both untreated and PMA-differentiated cells. Cytoinvasion of WGA-functionalized PLGA nanoparticles was additionally confirmed by fluorescence microscopy (Fig. 5). The images acquired after incubation at 37° revealed that the staining of the cytoplasm was not uniform but in a dot-like manner indicating vesicular accumulation of the particles. Thus, functionalisation of nanocarriers with WGA can lead to enhanced particle uptake into THP-1 cells. This is in line with Brandhonneur et al. [21] who recently showed increased uptake of WGA-grafted PLGA microparticles using pig alveolar macrophages. The specific interaction might be exploited for lectin-mediated drug delivery systems to combat infectious diseases evoked by parasites (malaria, leishmaniasis), facultative intracellular bacteria (brucella, liste-

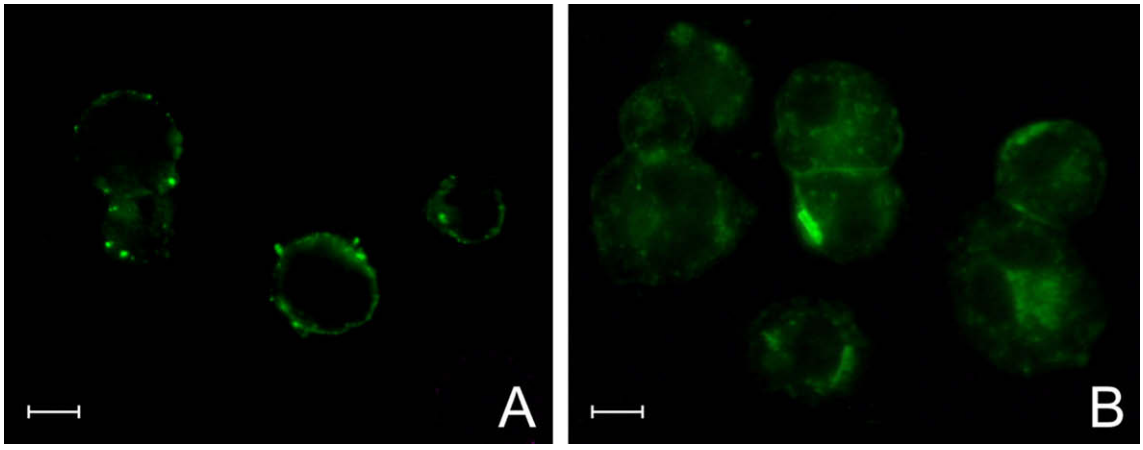

Fig. 5. Fluorescence microscopy images of differentiated THP-1 cells incubated with WGA-functionalized PLGA nanoparticles for 120 min at 4 °C (A) and 37 °C (B). Scale bar represents 10 μm

ria, shigella, mycobacteria), and viruses such as HIV which are known to colonize in the mononuclear phagocyte system [22,23].

In summary, the glycosylation pattern of THP-1 cells showed significant changes due to differentiation with PMA demonstrating a reorganization of sugar residues at the cell surface. Additionally, the endocytic capacity to free WGA and WGA-functionalised nanoparticles was higher in case of PMA-differentiated cells as compared to untreated cells, which might be a result of this rearrangement [4]. In this context, also the potential of WGA as a cytoinvasive vehicle was evaluated. Following on from this work, the application of WGA-grafted drug delivery systems might be an interesting approach towards treatment of diseases involving monocytes and macrophages which should be further pursued.

References

[1] H.S. Bennett, Morphological aspects of extracellular polysaccharides, J. Histochem. Cytochem. 11 (1963) 14–23.
[2] I. Carr, G. Everson, A. Rankin, J. Rutherford, The fine structure of the cell coat of the peritoneal macrophage and its role in the recognition of foreign material, Z. Zellforsch. Mikrosk. Anat. 105 (1970) 339–349.
[3] E.F. Hounsell, Glycobiology of the immune system, in: B. Ernst, G.W. Hart, P. Sinaÿ (Eds.), Carbohydrates in Chemistry and Biology, Wiley-VCH, New York, 2000, pp. 1029–1041.
[4] P.A. Videira, I.F. Amado, H.J. Crespo, M.C. Algueró, F. DalÍOlio, M.G. Cabral, H. Trinidade, Surface α2-3- and α2-6-sialyation of human monocytes and derived dendritic cells and its influence on endocytosis, Glycoconj. J. 25 (2008) 259–268.
[5] M. Soler, C. Merant, C. Servant, M. Fraterno, C. Allasia, J.C. Lissitzky, P. Bongrand, C. Foa, Leukosialin (CD43) behavior during adhesion of human monocytic THP-1 cells to red blood cells, J. Leukoc. Biol. 61 (1997) 609–618.
[6] S. Sabri, M. Soler, C. Foa, A. Pierres, A.M. Benoliel, P. Bongrand, Glycocalyx modulation is a physiological means of regulation cell adhesion, J. Cell Sci. 113 (2000) 1589–1600.
[7] S. Thomas-Ecker, A. Lindecke, W. Hatzmann, C. Kaltschmidt, K.S. Zänker, Alteration in the gene expression pattern of primary monocytes after adhesion to endothelial cells, PNAS 104 (2007) 5539–5544.
[8] S. Tsuchiya, M. Yamabe, Y. Yamaguchi, Y. Kobayashi, T. Konno, K. Tada, Establishment and characterization of a human acute monocytic leukemia cell line (THP-1), Int. J. Cancer 26 (1980) 171–176.
[9] S. Tsuchiya, Y. Kobayashi, Y. Goto, H. Okumura, S. Nakae, T. Konno, K. Tada, Induction of maturation in cultured human monocytic leukemia cells by a phorbol diester, Cancer Res. 42 (1982) 1530–1536.
[10] H. Schwende, E. Fitzke, P. Ambs, P. Dieter, Differences in the state of differentiation of THP-1 cells induced by phorbol ester and 1, 25-dihydroxyvitamin D3, J. Leukoc. Biol. 59 (1996) 555–561.
[11] Q. Chen, A.C. Ross, Retinoic acid regulates cell cycle progression and cell differentiation in human monocytic THP-1 cells, Exp. Cell Res. 297 (2004) 68–81.
[12] J. Auwerx, The human leukemia cell line, THP-1: a multifaceted model for the study of monocyte–macrophage differentiation, Experientia 47 (1991) 22–31.
[13] M. Kubin, J.M. Chow, G. Trinchieri, Differential regulation of interleukin-12 (IL-12), tumor necrosis factor α, and IL-1ß production in human myeloid leukemia cell lines and peripheral blood mononuclear cells, Blood 83 (1994) 1847–1855.
[14] E.K. Park, H.S. Jung, H.I. Yang, M.C. Yoo, C. Kim, K.S. Kim, Optimized THP-1 differentiation is required for the detection of responses to weak stimuli, Inflamm. Res. 56 (2007) 45–50.
[15] R. Gallily, B. Vray, I. Stain, N. Sharon, Wheat germ agglutinin potentiates uptake of bacteria by murine peritoneal macrophages, Immunology 52 (1984) 679–686.
[16] A. Weissenbock, M. Wirth, F. Gabor, WGA-grafted PLGA-nanospheres: preparation and association with Caco-2 single cells, J. Control. Release 99 (2004) 383–392.
[17] S. Takashiba, T.E. Van Dyke, S. Amar, Y. Murayama, A.W. Soskolne, L. Shapira, Differentiation of monocytes to macrophages primes cells for lipopolysaccharide stimulation via accumulation of cytoplasmic nuclear factor kappaB, Infect. Immun. 67 (1999) 5573–5578.
[18] D.L. Simmons, S. Tan, D.G. Tenen, A. Nicholson-Weller, B. Seed, Monocyte antigen CD14 is a phospholipid anchored membrane protein, Blood 73 (1989) 284–289.
[19] G. Maldonado, F. Porras, L. Fernández, L. Vázquez, F. Zenteno, Effect of lectins on mouse peritoneal macrophage phagocytic activity, Immunol. Invest. 23 (1994) 429–436.
[20] M. Wirth, C. Kneuer, C.M. Lehr, F. Gabor, Studying cellular binding and uptake of bioadhesive lectins, in: C.M. Lehr (Ed.), Cell Culture Models of Biological Barriers, Taylor and Francis, London and New York, 2002, pp. 62–93.
[21] N. Brandhonneur, F. Chevanne, V. Vié, B. Frisch, R. Primault, M.F. Le Potier, P. Le Corre, Specific and non-specific phagocytosis of ligand-grafted PLGA microspheres by macrophages, Eur. J. Pharm. Sci. 36 (2009) 474–485.
[22] C. Bogdan, Mechanisms and consequences of persistence of intracellular pathogens: leishmaniasis as an example, Cell. Microbiol. 10 (2008) 1221–1234.
[23] H.E. Gendelmann, M.S. Meltzer, Mononuclear phagocytes and the human immunodeficiency virus, Curr. Opin. Immunol. 2 (1989–1990) 414–419.